Concentric Tube Robots for Transurethral Prostate Surgery: Matching the Workspace to the Endoscopic Field of View

R. J. Hendrick[1], C. R. Mitchell[2], S. D. Herrell[2], R. J. Webster III[1]

[1]*Deparment of Mechanical Engineering, Vanderbilt University*

[2]*Department of Urologic Surgery, Vanderbilt Medical Center*

{richard.j.hendrick, christopher.r.mitchell, duke.herrell, robert.webster}@vanderbilt.edu

INTRODUCTION

Transurethral laser surgery using a flexible multi-backbone robot was recently demonstrated by Simaan et al. for bladder resection [1]. For transurethral prostate resection, thinner flexible manipulators are desirable. We have developed a hand-held system that transurethrally deploys two concentric tube robots through an 8.3 mm diameter rigid endoscope [2], as shown in Figs. 1 and 2. The purpose of this system is to facilitate Holmium Laser Enucleation of the Prostate (HoLEP), a surgery that is rarely used despite its demonstrated clinical benefits, because it is so challenging for the surgeon to perform [3]. The objective of the surgery is to remove prostate tissue transurethrally with a laser, and the challenge arises from the need to angulate the entire endoscope (impeded by a great deal of soft tissue) to aim the laser. Our system assists by providing one manipulator to aim the laser and a second to retract tissue, exposing desired targets to the laser.

The purpose of this paper is to explore optimal design of the concentric tube manipulators. We define an optimal design as one in which there is maximal overlap between the workspace of the manipulator and the space viewable by the endoscope. Here, we restrict our attention to the special case in which the concentric tube robot consists of two tubes, where the outer tube is straight and the inner tube is circularly curved. We note that more complex concentric tube manipulators are possible, such as the three tube robot shown in Fig. 2, but leave more complex cases to future work. Based on this, our objective is to choose (1) the curvature of the inner tube, and (2) the distance behind the camera lens inside the endoscope where the base of the workspace should occur.

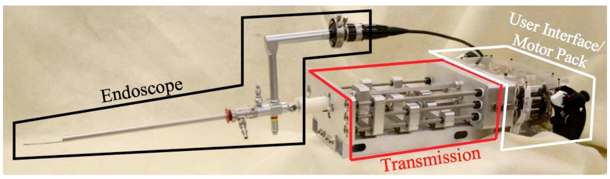

Fig. 1 This system is made up of three sections: a rigid endoscope that the manipulators pass through, a transmission where rotation and translation are applied to tube bases, and a user interface enabling the surgeon to control the endoscope and both manipulators. See [2] for a detailed description of this robot.

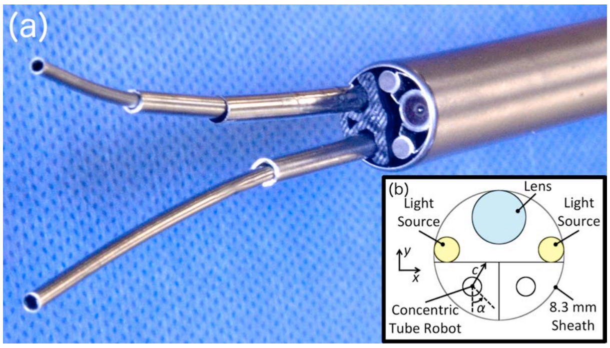

Fig. 2 (a) Two concentric tube manipulators are deployed through the 8.3 mm endoscope. One aims the laser fiber, and the other retracts tissue. (b) A cross section of the endoscope.

MATERIALS AND METHODS

The rigid endoscope mounted to our robotic system (Storz, Inc. 27292 AMA) delivers a camera lens and two fiber optic light sources through an 8.3 mm outer diameter sheath, with cross section illustrated in Fig. 2. This endoscope has a 6° angle of view, 103° field of view, 30 mm depth of view, and the lens is located 1.2 mm from the tip of the endoscope. Based on these specifications, the visualization volume is modeled as a cone with its vertex at the lens as shown in Fig. 3.

The manipulator that guides the laser fiber is currently the two-tube, 3-DOF robot. It has a straight, rigid stainless steel outer tube that can translate axially, and an elastic curved nitinol inner tube that can both translate and rotate axially. The forward kinematics for this simple manipulator can be computed analytically [2], and the workspace can be analytically described by a revolved circular arc with a cylinder appended (here we assume maximum arc length is limited to an arc that sweeps 90° and that the outer tube is perfectly rigid).

For the optimization, we place the robot exit point at the position within the endoscope cross section shown in Fig. 2. We note that this is not the only possible exit point (the tool channels shown in Fig. 2 are a design choice, not part of the endoscope), but it is roughly equidistant from the boundary defined by the endoscope sheath, a line tangent to the light sources, and the midline of the endoscope between the two manipulators. We denote the absolute tube rotation with α, the distance from the tube axis to the boundary with $c(\alpha)$, the radius of the inner tube with r (assumed to be 0.5 mm here), the curvature of the inner tube with κ, the

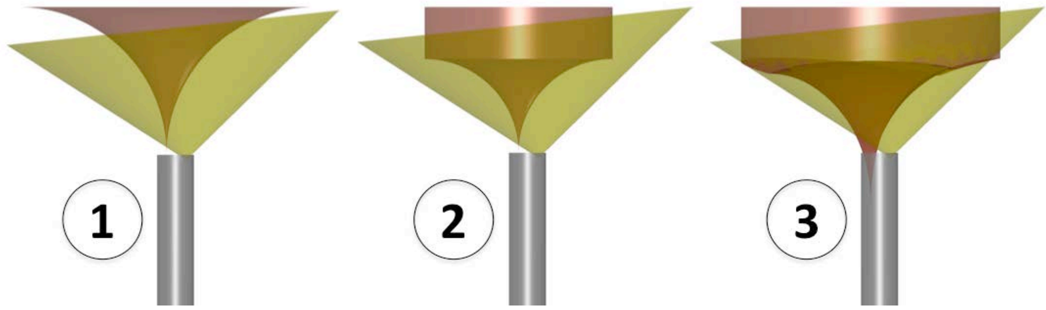

Fig. 3 Manipulator workspace (red) overlaid on visualization volume (yellow) for: (1) tube design (κ =30.1 m^{-1}, coverage=8.9%) in [2], (2) optimal design (κ =47.8 m^{-1}, coverage=29.5%) with workspace beginning at endoscope tip, and (3) optimal design (κ =34.6 m^{-1}, coverage=64.9%) when the workspace begins a short distance inside the endoscope.

angle subtended by the curved portion of the inner tube with θ, and the critical angle at which the inner tube collides with the boundary as θ_c. This angle and the distance behind the tip of the endoscope where the straight tube should end to achieve it, d, are given by:

$$\theta_c = \cos^{-1}\left(\frac{c\kappa - 1}{r\kappa - 1}\right)$$
$$d = \kappa^{-1}\sin(\theta_c).$$

From this, the trumpet-like workspace boundary, $\boldsymbol{b}$, can be shown to be

$$\boldsymbol{b} = \begin{pmatrix} -\kappa^{-1}\sin(\alpha)(\cos(\theta)-1) \\ \kappa^{-1}\cos(\alpha)(\cos(\theta)-1) \\ \kappa^{-1}\sin(\theta) - d \end{pmatrix},$$

where $\alpha \in [0\ 2\pi)$, $\theta \in [0\ \pi/2]$, and an origin on the tube axis at the endoscope tip is assumed. The closed curve defined at $\theta = 90°$ forms the bottom of a cylinder which extends out axially and forms the remainder of the workspace boundary (the cylindrical space can be accessed by extending both tubes together).

RESULTS

To choose the optimal curvature for the curved tube within a range of 20 to 70 m^{-1} we began by discretizing this range into 100 evenly spaced values. For each, the workspace was computed and the percentage of the visualization volume covered was determined. This was done by discretizing the visualization cone into 0.5 mm isotropic voxels, and counting as “covered” those voxels whose centers were inside the manipulator's workspace. Three different example cases of overlaid workspace and view volume are shown in Fig. 3 and view volume coverage as a function of curvature is shown in Fig. 4.

DISCUSSION

The value of optimizing tube design is illustrated by the ability to access a greater percentage of the endoscope visualization volume than the initial tubes in [2] could achieve. The most noteworthy result from this study is that placing the base of the workspace a short distance inside the endoscope is useful for reaching the maximum percentage of the visualization volume. To extend this design framework, one could consider also

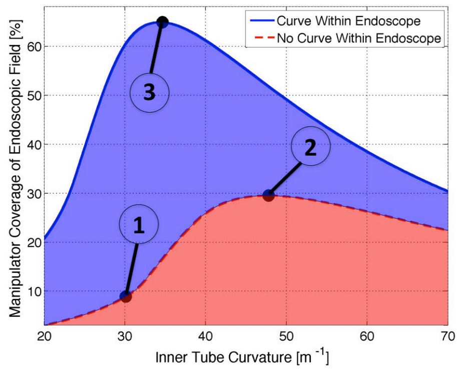

Fig. 4 Field of view coverage versus curvature. The labeled points correspond to the numbered illustrations in Fig. 3.

optimizing the exit location in the endoscope cross section, adding additional curved tubes to the manipulators, or using arc lengths beyond $\theta = 90°$. One could also consider using an endoscope with a different angle of view. Before studying these additional parameters, we intend to rigorously test the system in benchtop and cadaver experiments, to determine whether additional optimization variables are needed, and whether 3 DOF manipulators are sufficient to accomplish the surgery effectively and easily.

REFERENCES

[1] R. E. Goldman, A. Bajo, L. S. MacLachlan et al. Design and performance evaluation of a minimally invasive telerobotic platform for transurethral surveillance and intervention. IEEE Transactions on Biomedical Engineering. 2013;60(4):918-25.

[2] R. J. Hendrick, S. D. Herrell, and R. J. Webster III. A multi-arm hand-held robotic system for transurethral laser prostate surgery (in-press). IEEE International Conference on Robotics and Automation. 2014.

[3] J. E. Lingeman. Holmium laser enucleation of the prostate - if not now, when? The Journal of Urology. 2011 Nov;186(5):1762-63.

This work was funded in part by the National Science Foundation (NSF) under IIS-105433, in part by the National Institutes of Health (NIH) under R01 EB017467, and in part by the Vanderbilt Initiative in Surgery and Engineering. The content is solely the responsibility of the authors and does not necessarily represent the official views of the NSF or NIH.